Modeling Solid Sample Burning

GREGORY LINTERIS, LLOYD GEWUERZ, KEVIN MCGRATTAN, and GLENN FORNEY
Fire Science Division
National Institute of Standards and Technology
100 Bureau Dr. Stop 8665
Gaithersburg, MD 20899-8665

ABSTRACT

Black PMMA was burned in the cone calorimeter in two orientations (horizontal and vertical), at imposed radiant heat fluxes of (0, 5, 10, 25, 50, and 75) kW/m^2, and the visual appearance, flame size, heat release rate, and mass loss rate were recorded. Various other experimental parameters were varied. The topography of the burned samples was also recorded, and the heat flux to the sample was inferred from the variation of the mass loss over the surface of the sample. The burning was subsequently modeled using a computational fluid dynamics (CFD) model, and various experimental, numerical, and physical parameters were varied in the simulations. The results provide an indication of the ability of the fire model to predict the burning of a simple solid sample, and also provide guidance concerning the importance of various experimental and numerical parameters for accurate simulation.

KEYWORDS: direct numerical simulation of fire, cone calorimeter, fire modeling

INTRODUCTION

A number of CFD codes are available for predicting the movement of smoke and hot gases in building fires. Recently, their capabilities are being extended to include fire growth and spread. Predicting these phenomena is challenging, and experimental data are required to validate the code's accuracy. Clearly, intermediate and large-scale tests are required; however they are expensive and time consuming. It is also necessary to validate the sub-grid scale models with small-scale tests. The ultimate goal of the present work is to improve the treatment of flame spread on the solid phase in fire models. As a first step, small scale experiments were conducted in the NIST cone calorimeter and a fire model was used to predict the burning rate. This provides some measure of the model's capacity for predicting fire growth, since an ability to predict the burning of such a simple configuration is a clear prerequisite for modeling large fires which ultimately will also involve burning on the scale of cone samples. Hence, the short term goal of this project is to assess the relative importance of various numerical, physical, and experimental parameters on the predicted burning of the sample.

In order to avoid the complex phenomena which occur during the burning of some polymers (for example, bubbling, dripping, char formation, micro-explosions, complex time-dependent decomposition, etc.) [1], PMMA (a simple, well characterized and well behaved, non-charring, non-dripping polymer) was selected. Although it is desired to study these other parameters as well, their investigation will be conducted in future work, since their treatment is clearly beyond current modeling capabilities for burning samples.

In the experiments, the parameters varied include sample orientation (horizontal and vertical), radiant flux (0 to 75 kW/m^2), cone presence (for the 0 flux case), and the

FIRE SAFETY SCIENCE–PROCEEDINGS OF THE EIGHTH INTERNATIONAL SYMPOSIUM, pp. 625-636

sample edge and backing condition. In the numerical modeling, these parameters were varied, as well as those pertaining to the sample physical properties, and those relevant to the numerical solution (domain size, resolution, etc.).

EXPERIMENT

Black PMMA samples, (10 x 10 x 2.54) cm, were burned in the NIST cone calorimeter [2]. The samples had 6 cm of insulation on the back, and 0.77 mm thick cardboard around the perimeter. The heat release rate of the burning sample as a function of time was determined with oxygen consumption calorimetry (assuming a heat release of 13,125 kJ/kg-O_2); the mass loss rate and visual flame size were also recorded. The cone apparatus was modified so that the surface of the cone heater was always 2.54 cm from the burning PMMA sample (i.e., the cone was translated as the sample surface regressed). During the tests it was observed that the sample surface regression rate was non-uniform over the sample, and hence the sample final thickness as a function of position over the sample surface could be used to provide the integrated heat flux (or regression rate) for comparison with the numerical calculations. A custom-built system was used to measure the sample thickness as a function of position on the sample.

NUMERICAL CALCULATIONS

The burning of the cone samples was predicted with the NIST Fire Dynamics Simulator (FDS) version 4 [3], and the results interpreted with the companion visualization program Smokeview [4]. The low-Mach number formulation of the Navier-Stokes equations is solved to predict the gas movement. For PMMA combustion, the MMA monomer $C_5H_8O_2$ is assumed to be liberated from the sample surface when the surface is near an "ignition" temperature (based on a one-step Arrhenius rate expression). The rate of mass loss is determined from an energy balance at the surface, with all net incident energy generating MMA (accounted for with a "heat of vaporization"), with the PMMA treated as thermally thick. The code predicts the flame location based on a mixture fraction formulation, in which the fuel and oxygen consumption, as well as the heat release, occur in the grid cells for which the fuel and oxygen are present in stoichiometric proportions. Complete combustion at the flame sheet is assumed via the reaction: $C_5H_8O_2 + 6O_2 \Rightarrow 5CO_2 + 4\ H_2O$, (although slight modifications to the stoichiometric coefficients are made to account for empirically determined yields of soot and CO). Radiation heat transfer from hot surfaces (i.e., the cone and the hot surface of the PMMA) is calculated assuming unity emissivity; for the gases, gray body radiation is calculated (with a prescribed soot volume fraction and otherwise transparent gases; more details are available in ref. [3]). All boundaries of the calculation domain (except the sample) were open (ambient pressure).

In order to make the run times reasonable, the code was run primarily in the 2-D mode (planar for the vertical case, and axisymmetric for the horizontal case). Some 3-D calculations were also run for comparison, and to obtain the surface regression rate variation over the surface of the sample.

EXPERIMENTAL RESULTS

The data available from the experiments were flame visual images, the gas-phase heat release rate, and the sample mass loss rate, all as a function of time. In addition, the sample final mass and the topography of the burned samples were recorded. Images of

the flames from burning PMMA in the horizontal configuration are shown in Fig. 1 for imposed heat fluxes from the cone of: (0, 5, 10, 25, and 75) kW/m^2, together with the computational domain and a representative contour of peak heat release (right). The thick black horizontal stripe across the flame image (for all except the 0 flux case) is the cone heater (which occludes the flame).

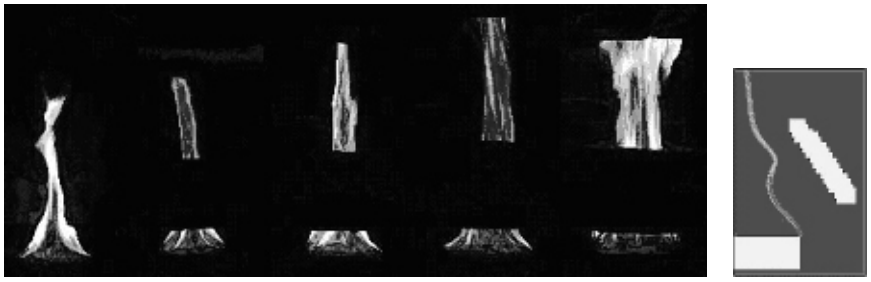

Fig. 1. Experimental (left) and calculated (right) horizontal flame images.

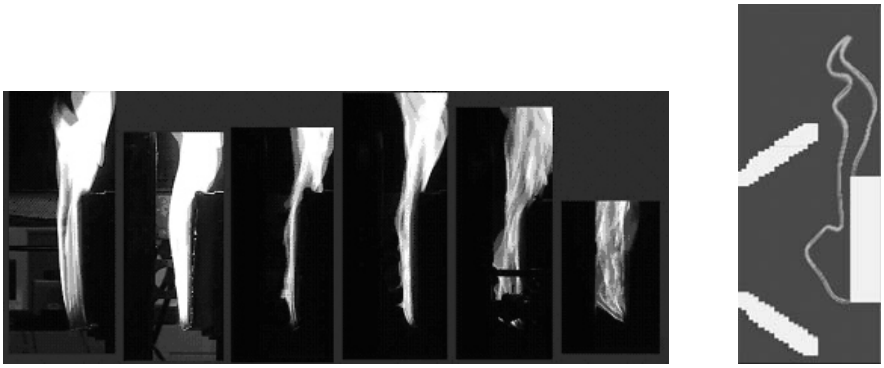

Fig. 2. Experimental (left) and calculated (right) vertical flame images.

The corresponding images for the vertical configuration are shown in Fig. 2 for imposed fluxes of (0, 5, 10, 25, 50, and 75) kW/m^2. In these images, the cone heater is just to the left of the flame (note that unfortunately, the camera view was different for the images in Fig. 2 so some flame images are clipped). The heat release rate as a function of time for the burning vertical and horizontal samples is shown in Fig. 3. As the figure shows, higher imposed heat fluxes lead to higher heat release rates and shorter ignition times; once ignited, the heat release increases rapidly, and the vertical and horizontal cases yield very similar heat release rates. (Note: the time to the start of the heat release represents the ignition time at that heat flux; however, for 0 and 5 kW/m^2, ignition would not occur, so the curves are shown on the plot transposed 200 s and 100 s, respectively, from the ignition time for the 10 kW/m2 case). The data also show that minor changes to the sample configuration can significantly influence the heat release rate. For example, for the 0 flux, horizontal case (labeled 0H), scraping the carbon left from the burned cardboard edge at the sample perimeter, or flipping the cold cone up or down, can each have about a 20% effect on the burning rate. These effects are discussed below.

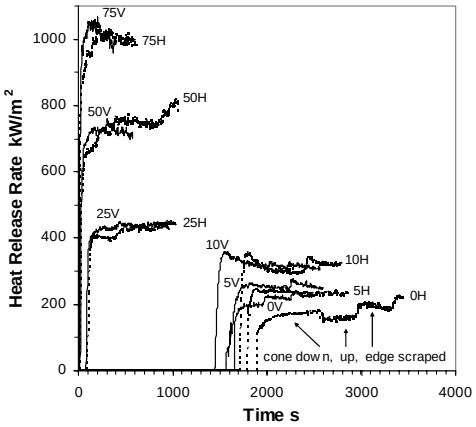

Fig. 3. Experimental heat release rate of horizontal H and vertical V PMMA in the cone calorimeter for imposed heat fluxes of 0 to 75 kW/m^2.

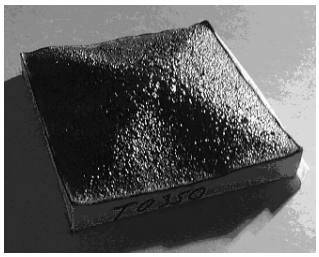

Fig. 4. Black horizontal PMMA sample exposed to 0 kW/m^2 for 26 min.

The samples did not burn uniformly over their exposed surface, and the effect was more pronounced at the lower flux levels. For example, the final condition of the horizontal sample at 0 kW/m^2 is shown in Fig. 4. From such samples, the burning rate variation over the surface of the sample can be determined.

NUMERICAL RESULTS

The calculations were performed at a Linux cluster at NIST, on 1.7 GHz to 3.2 GHz. Pentium 4 machines. The default domains used were 8 cm x 16 cm for horizontal and 27 cm x 6 cm for vertical orientations, with a grid size of 1 mm x 1 mm. Two-dimensional calculations in the horizontal or vertical orientation typically took 0.5 h or 1 h for 1 s of simulation, and 3-D calculations took 72 h per 1 s of simulation.

The baseline case input parameters for the reaction and surface properties of PMMA [5] are as follows: heat of vaporization 1578 kJ/kg; heat of combustion 25200 kJ/kg; sample thickness 0.025 m; thermal conductivity 0.25 Wm^{-1}K^{-1}; thermal diffusivity 1.1E-7 m^2/s; and sample initial temperature 330 K. Arrhenius rate parameters were selected to provide a sample mass flux of 0.004 kgs^{-1}m^{-2} at a temperature of 330 K, and the soot yield was specified to be 0.022 kg soot carbon /kg fuel.

The parameters varied in the calculations include those having to do with the numerical solution, the physical properties of the sample, and the experimental configuration that is modeled. The numerical parameters varied include the domain size, grid spacing, DNS or

LES calculation mode, and 2-D or 3-D calculation. The physical parameters varied were the heat of vaporization and the ignition temperature. The fidelity of the experimental description in the calculation was varied by including or excluding such effects as the presence of the exhaust flow, the lip on the sample edge, presence of the cone above the sample (in the no-flux case), and the sample backing insulation. Finally, the major experimental parameters were varied by changing the cone temperature (i.e., the imposed heat flux), and the sample orientation (horizontal or vertical). The effects of each of these parameters on the predicted heat release rate are described below.

Numerical Parameter Variation

The domain size had a large effect on the heat release occurring in the gas phase. A plot of the calculated heat release rate (HRR) in the system as a function of time is shown in Fig. 5 as the circles. (Since the heat is released in the gas phase, this HRR will be referred to as the gas-phase HRR. Conversely, one can calculate

HRR from the solid-phase mass loss rate times the heat of combustion; this will be referred to as the solid-phase HRR. Note that in the calculations, no actual energy is released within the solid phase; this naming convention merely refers to how the HRR is estimated.) The solid-phase HRR is shown by the lines. There is large scatter in the gas-phase HRR, as well as significant discrepancy between the average of the gas-phase and solid-phase results, with the solid-phase HRR about 40% higher than the average of the gas-phase HRR. Examination of the heat release contours indicated that the limited physical domain leads to loss of reactants before they are consumed, leading to a lower HRR than indicated by the burning rate (which counts all vaporized fuel as burned). For the calculation shown by the (+) symbols and indicated lines, the physical domain was increased by a factor of 4 in the direction perpendicular to the horizontal sample (i.e., up). With the larger domain, there is less scatter in the gas-phase HRR, the average of the gas-phase and solid-phase HRR agree better with each other, and the solid-phase HRR is about 10% lower than that calculated for the original domain.

For vertical samples, the results were similar: a larger domain leads to better agreement between the HRR predicted from the gas phase and the solid phase, and leads to a slightly lower heat release predicted by the solid-phase mass loss. For the vertical case, however, even with the larger domain, there is still a 10% discrepancy between the average HRR predicted from the gas phase as compared to the solid phase, indicating that a still larger domain may be necessary. Note that some of this discrepancy between the mass loss-based HRR and that calculated to occur in the gas phase may also be numerically induced.

The grid spacing selected was very important, but the results were counter-intuitive. For the vertically-oriented PMMA sample, calculations were performed using a grid spacing of either 1 mm or 2 mm (in both the x and z directions). With a lower resolution, the gas-based and solid-based HRR tend to converge and the gas-based rate shows less variation. (These effects may be numerically induced). More importantly, the results of the calculations indicate a significant drop in heat release rate (about a factor of two) for the coarser grid.

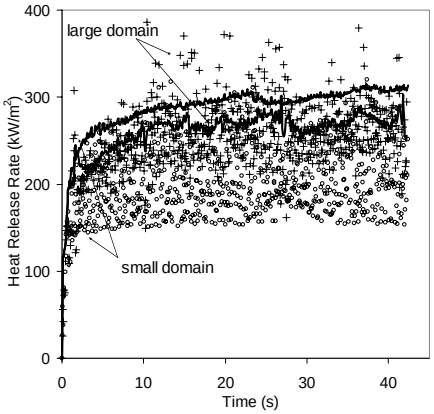

Fig. 5. Heat release in gas phase (points), or based on solid phase mass loss rate (lines) with original small(o) or larger(+) domain.

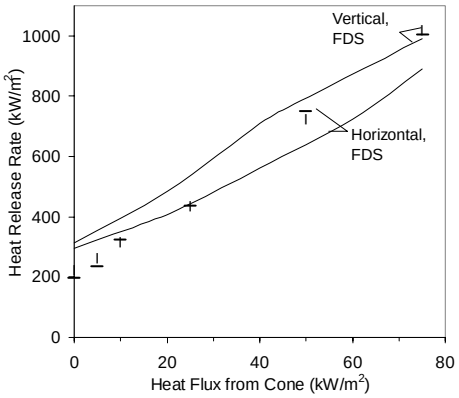

Fig. 6. Experimental (points) and simulated (lines) heat release rate from PMMA in cone.

Two types of calculations were performed: Large Eddy Simulation (LES) and Direct Numerical Simulation (DNS), differing in their treatment of the sub-grid-scale dynamic viscosity term of the momentum equation. Although the grid resolution is fine enough for the present calculations that there may not be much difference between the two, we ran calculations in both modes. Also, in large-scale LES calculations with FDS, the baroclinic vorticity term in the momentum equation is typically ignored (a reasonable simplification for larger-scale calculations). For the present small-scale application, however, inclusion of the baroclinic vorticity term does affect the results, and hence we performed LES calculations with and without this term. The LES case without baroclinic vorticity predicted the HRR to be a few percent higher than the DNS case, while surprisingly, the LES case with baroclinic vorticity predicted HRR 7% and 16% higher than DNS case for the horizontal and vertical orientations, respectively.

All of the previous simulations were performed using a two-dimensional analysis. Three dimensional calculations are also possible (with run times increased by a factor of about 100). One case for each of the horizontal and vertical sample scenarios (each burning with zero imposed flux from the cone) was calculated in three-dimensional mode. For the

horizontal sample, there is not much variation in the heat release rate as the simulation mode is changed. Therefore, the faster, two-dimensional mode appears to be sufficiently accurate. More of a difference is evident for the vertical orientation, with the two-dimensional mode predicting a 7% lower heat release rate. This lower HRR in the 2-D mode for the vertical samples may be due to edge effects: the actual samples (as well as the 3-D calculation) show significant burning at the lateral edges of the samples that is not captured in the 2-D planar (i.e., infinite length, no edges) calculation. Since the horizontal 2-D calculation is done in the axisymmetric mode, it has a complete edge and would not experience this inaccuracy.

Physical Parameter Variation

The physical parameters necessary for predicting the burning rate are the specific heat, thermal conductivity, density, heat of combustion, heat of vaporization (i.e., decomposition), and kinetic parameters describing the mass loss rate as a function of temperature. In the numerical tests, we varied the heat of vaporization and the ignition temperature (i.e., the characteristic temperature at which mass loss occurs).

To determine the effect of the heat of vaporization, calculations for a horizontal sample were run using values of 1578 kJ/kg (baseline case) and 1420 kJ/kg (10% reduced) for this parameter. Both cases were run with an imposed heat flux of 0 kW/m^2 and 75 kW/m^2. A lower heat of vaporization produced a higher heat release rate. This is expected since the mass loss rate $\dot{m}''$ is equal to the ratio of the net heat flux to the heat of vaporization, $\frac{\dot{q}''_{net}}{L_v}$, and the HRR is the product of the mass loss rate and the heat of combustion of PMMA. The difference between the baseline case and the 10% lower heat of vaporization was slightly more significant in the high flux case (approximately 8%) than in the no flux case (approximately 5%). To first order, since all of the heat released goes into vaporizing the PMMA, a 10% decrease in L_v is expected to give a 10% increase in burning rate; however, some of the heat feedback to the sample surface also goes into conductive losses which are a larger fraction of the total heat flux to the sample for the 0 imposed flux case. This may explain the lesser effect for the no flux case.

For horizontal PMMA, decreasing the heat of vaporization improved agreement with the experiment somewhat, especially for the higher fluxes. For the vertical cases, however, lowering the heat of vaporization 10% may not improve the prediction, since the calculated heat release rate is fairly close to the measured value at 75 kW/m^2, and lowering the heat of vaporization would increase the heat release rate at that flux (see Fig. 6).

The temperature at which the sample vaporizes (like a boiling point for a liquid fuel) is referred to here as the "ignition temperature." A higher ignition temperature decreases the heat transfer rate to the sample by convection, and increases the heat loss rate by radiation. We varied the ignition temperature of PMMA by ± 50ºC around the literature value of 330ºC, for horizontal PMMA burning with an imposed flux of 0 and 75 kW/m^2. A 100ºC increase in the ignition temperature gives a 10% drop in the mass loss rate for the high-flux case, and a 15% drop for the low flux case. The heat loss by radiation $\dot{q}''_{r,loss}$ can be estimated from the radiation heat transfer equation $q''_{r,loss} = \varepsilon\sigma(T_s^4 - T_{amb}^4)$, which can then be compared with the net heat flux into the

sample $\dot{q}''_{net}$. The net heat flux $\dot{q}''_{net}$ can be estimated from the heat release rate $\dot{q}''_{rel}$ since $\dot{q}''_{rel} = \dot{m}'' \cdot \Delta H_C$ and $\dot{q}''_{net} = \dot{m}'' \cdot L_v$, in which ΔH_C is the heat of combustion and L_v is the heat of vaporization. From Fig. 6, the predicted heat release rate for incident radiant fluxes of 0 kW/m^2 and 75 kW/m^2 is about 310 kW/m^2 and 890 kW/m^2, respectively, which implies a net heat input going to pyrolysis of 19 kW/m^2 and 56 kW/m^2. For surface temperatures of 280ºC and 380ºC, the predicted radiant heat loss is 5.3 kW/m^2 and 10.3 kW/m^2 , or a difference of about 5 kW/m^2 between 280ºC and 380ºC. Hence, the 5 kW/m^2 higher heat losses is about the right magnitude for the high-flux case (about 10% of the total energy going into pyrolysis), but too high (by a factor of two) for the low-flux case. That is, the lower burning rate of the low-flux case caused by a higher ignition temperature is not as low as one would expect based just on the higher radiative losses at the higher temperature. (Note that in the calculation, the outer edge of the PMMA is specified as non-burning, and is set to the same temperature as the ignition temperature, so lateral conductive losses are not the reason for the lower burning rate at the higher ignition temperature.)

Experimental Parameter Variation

Several of the experimental parameters had little effect. Calculations for a vertical sample at an imposed flux of 10 kW/m^2 indicated that presence of insulation on the back of the sample had no significant effect (the thermal time constant of the sample was 1 h to 2 h, but the simulation ran for only 60 s). Experiments with runs times of about 20 min also showed no effect. The influence of the exhaust vent also showed no effect. Calculations performed with an imposed 15 cm/s upper boundary flow (simulating the mass flow from the exhaust hood [2]) showed no significant difference from the base case with only natural convection.

Calculations were performed with and without the presence of a cone heater. For these calculations, the cone had no heat capacity, so the effects are only due to changes to the flow-field, and to the radiant heat feedback from the un-powered cone. In the experiment, when the cone was positioned above the burning horizontal sample, the flame gases heated it to about 102ºC. Hence, in the simulation, its temperature was set to either 20ºC for checking the effect on the flow-field, or to 110ºC to assess changes to the radiant feedback. In the calculated result, there is very little difference between the warm and cold cone, and only a 3% difference between them and the case with the cone absent. For the vertical case, the calculations predict an 8% increase in the burning rate with the cone removed. The lack of effect of the warm vs. cold cone is consistent with the small magnitude of the radiation from the cone at these temperatures (the cone flux at 110ºC is about 5% of the heat flux from the flame to the PMMA surface). In contrast, the experiment showed a large difference with the cone present or removed. As shown in Fig. 3, removing the cone from the horizontal sample decreased the HRR 18% rather then the few percent increase predicted by the calculations.

Edge effects in the cone sample are known to affect the burning rate [6]. In the actual cone calorimeter experiments, the PMMA sample is surrounded by a cardboard strip. As the sample burns, a “lip” of char from the cardboard builds up around the edges and is either left in place or scraped away. This scraping has a significant effect on the heat release rate of the sample, as shown in Fig. 3, which indicates a 20% higher burning rate when the lip is scrapped away. This was simulated by creating a thin inert lip at two and four millimeters above the sample surface and giving it a constant temperature equal to

the ignition temperature of the PMMA (330ºC). The results show that 2 mm and 4 mm lips reduce the burning rate by 25% and 40%. This is consistent with the size of the lip formed during the experiment, and the magnitude of the increase in burning rate after removing the lip (as shown in Fig. 3).

Heat Flux from the Cone

The major parameter varied in both the experiments and the calculations was the imposed radiant flux on the PMMA sample. In the experiments, this was achieved by adjusting the cone temperature until a calibrated Schmidt-Boelter heat flux gage indicated the desired heat flux (tests were run at 0, 5, 10, 25, 50, and 75 kW/m^2). Similarly, in the calculations, the cone temperature was selected to provide the desired flux on the sample.

Fig. 6 shows the heat release rate from vertical (|) and horizontal (—) PMMA as a function of imposed heat flux from the cone; the experimental data are shown by the points, and the prediction by the solid lines. A somewhat surprising result is that in the experiment, the horizontal and vertical cases provide essentially the same burning rate for the vertical and horizontal cases, even down to 0 kW/m^2 imposed flux.

The model is able to predict the burning rate reasonably for both cases, although the increase in heat release rate with imposed flux (i.e., the slope of the line in the figures) is less in the calculations than in the experiment, especially for the horizontal case. The slope of this line can be modified slightly by changing the heat of vaporization for PMMA; however, this would make the agreement for the vertical case worse. For both orientations, the poorest agreement occurs for the case of 0 kW/m^2 imposed flux. Reasons for this are discussed below.

Surface Mass Loss Variation

As described above, the non-uniform PMMA samples obtained at the conclusion of each burn provide the opportunity to estimate the burning rate variations over the surface of the samples. The surface topography of the PMMA samples was determined with an automated system, and results are presented for the 0 kW/m^2 horizontal and vertical cases in the left image of Fig. 7 and Fig. 8, respectively (more data are available in ref. [7]). For either orientation, higher imposed fluxes lead to greater fuel consumption and a more uniform burning over the surface of the sample (the heat transfer at higher imposed flux is dominated by the thermal radiation from the cone, which is uniform). Since the 0 kW/m^2 imposed flux case has the largest variation in mass loss rate over the surface, these are compared with predictions.

The right images in Fig. 7 and Fig. 8, show the 3D-prediction of the surface height (based on mass loss rate to a planar surface) for 0 kW/m2 imposed flux. Since the numerical simulations for the 3-D calculations only ran for about 30 s or less of burning time (which took several months in real time), it was necessary to extrapolate these results for longer burn times to produce a sample topography similar to the experimental results (which had burn times of hundreds of seconds). To do this, we first determined the average burning rate over the surface of the sample for the last second of the calculation. Then, the burning time for the simulation was selected to give the same final mass of the experiments. With this integration time, the mass loss at each location on the surface was calculated based on the surface variation of the mass loss rate predicted by the 3-D calculation. This approach was used since: 1.) the calculation time for the 3-D simulation was very long, and we could not achieve the actual burning times in the time available for

the calculations, and 2.) the modeling results for the average steady-state burning rate at 0 kW/m^2 flux was about 80% too high (see Fig. 6 at 0 kW/m^2), so using actual burning times would not give the proper total mass loss. While not quantitative, the approach used (selecting the burn time in the calculations to match the experimental mass loss) allows us to assess the overall ability of the code to predict the *distribution* of surface erosion. As shown, the simulation is able to capture the trends in the surface variation. The burning of the middle of the horizontal sample, however, is too large and the gradient at the edges is too steep. For the vertical sample, the gradient of the mass loss rate at the edges is again much more gradual in the experiment as compared to the model. Nonetheless, there is a limit to the agreement between calculation and experiment in these cases since the code does not allow changes to the sample geometry during burning. Hence, local changes to the heat transfer coefficient caused by changes to the shape of the sample, which would occur in the experiment but not in the calculation, may be responsible for the discrepancies observed here.

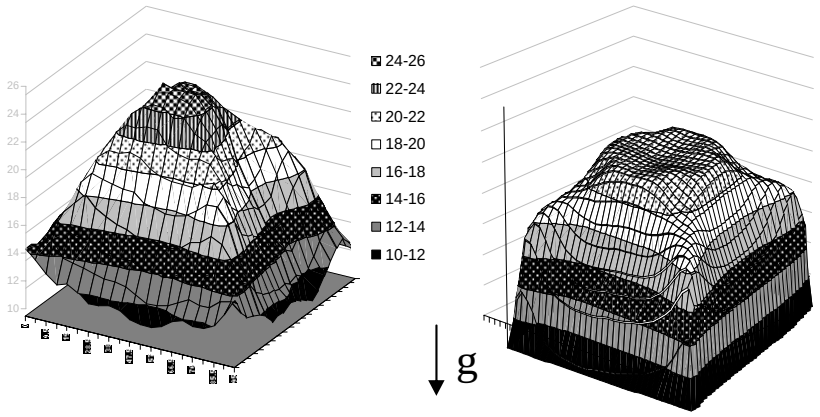

Fig. 7. Experimental (left) and numerically predicted (right) topography of horizontal PMMA at 0 kW/m^2 imposed flux. Experiment 1560 s run time; simulation, 819 s.

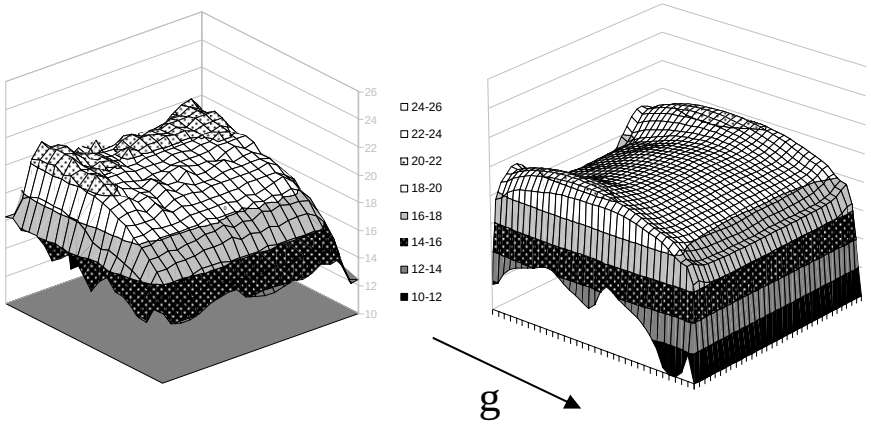

Fig. 8. Experimental (left) and numerically predicted (right) topography of vertical PMMA at 0 kW/m^2 flux; g: gravity. Experiment 825 s run time; simulation, 485s.

CONCLUSIONS

A computational fluid dynamics code was used to simulate the burning of black PMMA samples in the cone calorimeter. Various parameters were found to have a large effect on either the experimental or calculated burning rates, and must be carefully controlled in the experiment or modeling. In the calculations, numerical parameters, physical, and experimental parameters were varied.

Numerical Parameters:

1. The domain size and grid resolution were both found to have a large effect, especially on the heat release rate in the gas phase.
2. The selection of DNS or LES mode did not make much difference for the present calculations (with 1 mm grid size).
3. The 2-D simulation (axisymmetric) was within a few percent of the 3-D calculation for horizontal samples, while the 2-D planar simulation for the vertical samples was about 7% lower than the 3-D simulation.

Physical Parameters:

1. Heat of vaporization, ignition temperature, and activation energy of the decomposition step all had a significant effect (about 10%) on the burning rate over a range of variation of their values which may be observed in practice.

Experimental Parameters:

1. The presence or absence of the cone (with 0 kW/m^2 flux) above the horizontal sample was important in the experiment, but not important in the calculations.
2. The presence of the exhaust flow in the hood above the cone was not important in the calculations.
3. The presence of insulation on the back side of the sample was not important in either.
4. The presence of a lip on the sample edge was important in both the experiments and calculations, with a 4 mm lip changing the burning rate by almost a factor of two.
5. The variation in the average sample burning rate with changes to the imposed flux (over the range of 0 kW/m^2 to 75 kW/m^2) was predicted reasonably well by the simulations; however, as the imposed flux went down, the simulation overpredicted the average mass loss rate as compared to the experiment
6. For the 0 kW/m^2 imposed flux case, most of the heat flux from the flame to the sample occurs at the edges; however, the code over-predicts heat flux both in the center and at the edges.

The reasons for this over-prediction of the burning rate with no imposed flux are related to the fidelity with which the phenomena were set up in the numerical description. In the center, the heat flux is mainly by radiation, and the calculation was greatly simplified. Only gray-body radiation from an assumed soot volume fraction was included, and this may be in error. Gas-phase species were not included, and in particular, absorption of the IR radiation by the pyrolyzed but unburned MMA monomer is known to have an effect. Treatment of the edge condition may need to be improved, and the changes to the sample geometry during burning (not included in FDS) could affect the result. As the imposed heat flux from the cone increases, it dominates the heat flux to the sample, so flame

radiation and edge heat transfer effects are not so important (although absorption of the radiation by the MMA monomer, or its decomposition products, could still be important).

In future work, it would be useful to look at the time dependence of all of the results generated in the present work, since only the steady-state results were analyzed in the present discussion. Further, it would be of interest to study more complex solid fuels, for which the present capabilities of the code for treating the solid phase would clearly need to be upgraded. Nonetheless, the present results are an invaluable foundation for understanding how the myriad experimental and numerical parameters which can be manipulated in the tests and the analyses affect the accuracy of the comparisons between calculations and experiment.

ACKNOWLEDGEMENTS

The authors are indebted to Dr. Richard Lyon of the FAA Technical Center for his initial calculations and experiments which motivated this work, and to Mr. Randy Shields and Mr. Ian Rafferty for the experiments and data reduction. Helpful conversations with Dr. William (Ruddy) Mell concerning PMMA modeling are gratefully acknowledged.

REFERENCES

[1] Kashiwagi, T., "Polymer Combustion and Flammability-Role of the Condensed Phase," *Proc. Combust. Inst.* **25**: pp. 1423, (1994).

[2] Twilley, W.H. and Babrauskas, V., "User's Guide for the Cone Calorimeter," National Institute of Standards and Tech., SP-745, Gaithersburg, MD, 1988, p. 125.

[3] McGrattan, K.B., "Fire Dynamics Simulator (Version 4) Technical Reference Guide," NIST, NISTSP 1018, Gaithersburg, MD, 2004, p. 97.

[4] Forney, G.P. and McGrattan, K.B., "User's Guide for Smokeview Version 4 - A Tool for Visualizing Fire Dynamics Simulation Data," NIST, NISTSP 1017, Gaithersburg, MD, 2004, p. 96.

[5] Tewarson, A., "Experimental Evaluation of Flammability Parameters of Polymeric Materials," Factory Mutual Research Corp., FMRC J.I. 1A6R1.RC, Norwood, MA, 1979.

[6] Babrauskas, V., Twilley, W.H., and Parker, W.J., "The Effects of Specimen Edge Conditions on Heat Release Rate," *Fire and Materials*, **17**: p. 51, (1993).

[7] Linteris, G.T., "Modeling Solid Sample Burning with FDS," National Institute of Standards and Technology, NISTIR 7178, Gaithersburg MD, 2004, p. 36.